Systems & Control Letters 57 (2008) 805–812

Contents lists available at ScienceDirect

Systems & Control Letters

journal homepage: www.elsevier.com/locate/sysconle

Stabilization of linearized 2D magnetohydrodynamic channel flow by backstepping boundary control

Chao Xu [a,*], Eugenio Schuster [a], Rafael Vazquez [b], Miroslav Krstic [b]

[a] Department of Mechanical Engineering and Mechanics, Lehigh University, 19 Memorial Drive West, Bethlehem, PA 18015, USA
[b] Department of Mechanical and Aerospace Engineering, University of California, San Diego, La Jolla, CA 92093, USA

ARTICLE INFO

Article history:
Received 13 November 2006
Received in revised form
20 August 2007
Accepted 14 March 2008
Available online 23 May 2008

Keywords:
Magnetohydrodynamics
Boundary stabilization
Backstepping technique

ABSTRACT

We present a boundary control law that stabilizes the Hartman profile for low magnetic Reynolds numbers in an infinite magnetohydrodynamic (MHD) channel flow. The proposed control law achieves stability in the L^2 norm of the linearized MHD equations, guaranteeing local stability for the fully nonlinear system.

1. Introduction

A backstepping boundary control law is proposed for stabilization of the 2D linearized magnetohydrodynamic (MHD) channel flow, also known as Hartmann flow. This flow is characterized by an electrically conducting fluid moving between parallel plates in the presence of an externally imposed transverse magnetic field. The system is described by the MHD equations which is a combination of the Navier–Stokes equations and the Maxwell equations.

While control of flows has been an active area for several years, up until now active feedback flow control developments have had little impact on electrically conducting fluids moving in electromagnetic fields. Prior work in this area focuses mainly on electro-magneto-hydro-dynamic (EMHD) flow control for hydrodynamic drag reduction, through turbulence control, in weak electrically conducting fluids such as saltwater. Traditionally two types of actuator designs have been used: one type generates a Lorentz field parallel to the wall in the streamwise direction, while the other one generates a Lorentz field normal to the wall in the spanwise direction. EMHD flow control has been dominated by strategies that either permanently activate the actuators or pulse them at arbitrary frequencies. However, it has been shown that feedback control schemes, making use of "ideal" sensors, can improve the efficiency, by reducing control power, for both streamwise [19] and spanwise [5,4] approaches. From a model-based-control point of view, feedback controllers for drag reduction are designed in [2,16] using distributed control techniques based on linearization and model reduction. Prior work can also be found in the area of mixing enhancement. In [15], a controller, designed using Lyapunov methods, that does not rely on linearization or any type of model reduction is proposed for optimal mixing enhancement by blowing and suction. In [1], they discussed optimal perturbations to a magnetohydrodynamic flow bounded by perfectly insulating or conducting walls and the energy growth mechanisms with respect to parameters of the Hartmann flow.

The stability of conducting fluids under the presence of a magnetic field was studied extensively in [20,11,13,24]. The method used in this paper for stabilizing the linearized 2D MHD equations is based on the recently developed backstepping technique for parabolic systems [17], which has already been successfully applied to the stabilization of 2D and 3D linearized Navier–Stokes channel flows [22,6].

We organize this paper as follows. In Section 2 the mathematical model of the MHD channel is stated, the equilibrium profiles are obtained, and the MHD equations are linearized around these equilibrium profiles. Then we convert the linearized MHD equations into the wave-number space (frequency domain, or Fourier space) by using the Fourier transform technique. This approach allows separate analysis for each wave number, as all pairs are uncoupled from each other. The wave numbers are split into two sets. For the first set, the controlled set, a normal velocity controller is designed in Section 3 to put the system into a form where a linear Volterra operator, combined with boundary feedback for the

* Corresponding author. Tel.: +1 610 758 3707.
E-mail addresses: chx205@lehigh.edu (C. Xu), eus204@lehigh.edu (E. Schuster).

0167-6911/$ – see front matter © 2008 Elsevier B.V. All rights reserved.
doi:10.1016/j.sysconle.2008.03.008

tangential velocity, can transform the original normal velocity PDE into a stable heat equation. For the second set, the uncontrolled set, the system is proved to be open loop exponentially stable in Section 4. In addition, the stability of the system is proved for the controlled set of wave numbers. Combining these two results, stability of the closed loop system is proved for all wave numbers in the wave-number space and in the physical space. In Section 5 we close the paper with some concluding remarks and discussion of the future work.

2. Model

2.1. Governing equations

We consider the flow of an incompressible, Newtonian (constant viscosity), conducting fluid between parallel plates where an external magnetic field perpendicular to the channel axis is applied. This flow was first investigated experimentally and theoretically by Hartmann [8]. The dimensionless governing equations include the momentum transport equation,

$$\frac{\partial \mathbf{v}}{\partial t} + (\mathbf{v}\cdot\nabla)\mathbf{v} = -\nabla P + \frac{1}{R}\nabla^2\mathbf{v} + N(\mathbf{j}\times\mathbf{B}), \tag{1}$$

and the magnetic induction transport equation,

$$\frac{\partial \mathbf{B}}{\partial t} = \nabla\times(\mathbf{v}\times\mathbf{B}) + \frac{1}{R_m}\nabla^2\mathbf{B}, \tag{2}$$

where $\mathbf{v}$ is the velocity field of the fluid, $\mathbf{B}$ is the magnetic field, $\mathbf{j}$ is the current density, and P is the pressure. R, R_m, and N are the Reynolds number, magnetic Reynolds number, and Stuart (or interaction) number, respectively. The current density is given by Ampere's law,

$$\mathbf{j} = \frac{1}{R_m}\nabla\times\mathbf{B}. \tag{3}$$

Both $\mathbf{B}$ and $\mathbf{v}$ are solenoidal,

$$\nabla\cdot\mathbf{B} = 0, \tag{4}$$

$$\nabla\cdot\mathbf{v} = 0. \tag{5}$$

In this work, we consider MHD flow at low magnetic Reynolds number R_m [10]. When $R_m \ll 1$, the induced magnetic filed is very small in comparison with the applied magnetic field. Since the applied magnetic field $\mathbf{B}_0$ is assumed to be static, then $\frac{\partial \mathbf{B}}{\partial t} = 0$ and $\mathbf{B} \approx \mathbf{B}_0$ in (2). In this case, Ohm's law becomes

$$\mathbf{j} = -\nabla\phi + \mathbf{v}\times\mathbf{B}_0, \tag{6}$$

where ϕ is the electric potential. Since $\mathbf{j}$ is a solenoidal field, a Poisson equation is obtained for ϕ by computing the divergence of Ohm's law (6). The governing equations of the system become

$$\begin{aligned}\frac{\partial \mathbf{v}}{\partial t} + (\mathbf{v}\cdot\nabla)\mathbf{v} \;=\; & -\nabla P + \frac{1}{R}\nabla^2\mathbf{v} + N(\mathbf{v}\times\mathbf{B}_0)\times\mathbf{B}_0 \\ & - N(\nabla\phi\times\mathbf{B}_0),\end{aligned} \tag{7}$$

$$\nabla^2\phi = \nabla\cdot(\mathbf{v}\times\mathbf{B}_0) = \mathbf{B}_0\cdot\omega, \tag{8}$$

$$\nabla\cdot\mathbf{v} = 0, \tag{9}$$

where $\omega = \nabla\times\mathbf{v}$ is the vorticity. Eqs. (7)–(9) are referred to as the simplified magnetohydrodynamic equations (SMHD). For the 2-D Hartman flow considered in this work, whose geometrical configuration is illustrated in Fig. 1 ($(x, y) \in (-\infty, \infty)\times[0, 1]$), we write $\mathbf{v}(t, x, y) = U(t, x, y)\hat{\imath} + V(t, x, y)\hat{\jmath}$, $\mathbf{B}_0(t, x, y) = B_0(t, x, y)\hat{\jmath}$ and $P = P(t, x, y)$, then

$$(\mathbf{v}\times\mathbf{B}_0)\times\mathbf{B}_0 = -B_0^2 U\hat{\imath}, \tag{10}$$

$$\nabla\phi\times\mathbf{B}_0 = (\phi_x\hat{\imath} + \phi_y\hat{\jmath})\times B_0\hat{\jmath} = \phi_x B_0\hat{k}, \tag{11}$$

$$\omega = \nabla\times\mathbf{v} = \left(\frac{\partial V}{\partial x} - \frac{\partial U}{\partial y}\right)\hat{k}, \tag{12}$$

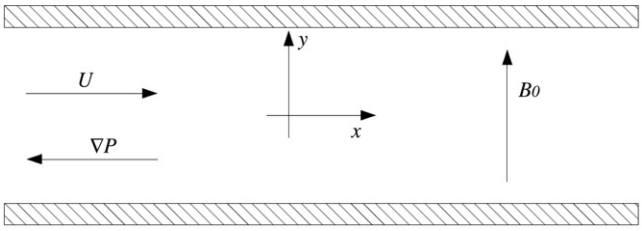

Fig. 1. 2D Hartman flow.

where $\hat{\imath}$, $\hat{\jmath}$ and $\hat{k}$ are the unit vectors of the Euclidean coordinate system employed here. For the last term $\nabla\phi\times\mathbf{B}_0$ in (7), the only component remaining, $\phi_x B_0$, lies in z-direction. Since we consider a 2D geometry,

$$\phi_x(x, y) = 0. \tag{13}$$

Therefore, the Poisson equation (8) for the electric potential $\phi(x, y)$ reduces to a degenerated ordinary differential equation, $\phi_{yy}(x, y) = 0$. Integrating it twice, we obtain

$$\phi(x, y) = C_1(x)y + C_2(x). \tag{14}$$

Differentiating with respect to x, and recalling (13), we obtain

$$C_1'(x)y + C_2'(x) = 0, \quad \forall(x, y) \in (-\infty, \infty)\times[0, 1]. \tag{15}$$

Evaluating this last expression at $y = 0$ and $y = 1$ respectively, we conclude that C_1 and C_2 must be constants. Assuming non-conducting walls, i.e.

$$\phi_y|_{y=0,1} = 0, \tag{16}$$

then we can determine $\phi(x, y)$ as a constant potential field. The SMHD Eqs. (7)–(9) can be written now as

$$U_t + UU_x + VU_y = -P_x + \frac{1}{R}(U_{xx} + U_{yy}) - NB_0^2 U, \tag{17}$$

$$V_t + UV_x + VV_y = -P_y + \frac{1}{R}(V_{xx} + V_{yy}), \tag{18}$$

$$U_x + V_y = 0, \tag{19}$$

with boundary conditions

$$U = 0, \qquad V = 0, \quad \text{at } y = 0, \quad \forall x \in (-\infty, \infty), \tag{20}$$

$$U = U_c, \qquad V = V_c, \quad \text{at } y = 1, \quad \forall x \in (-\infty, \infty), \tag{21}$$

where U_c, V_c are the boundary controls. In order to compute the equilibrium state we put the boundary controls be zeros, i.e.

$$U = 0, \quad V = 0, \quad \text{at } y = 0, 1, \forall x \in (-\infty, \infty). \tag{22}$$

By differentiating (17) and (18) with respect to x and y, respectively and recalling the incompressibility condition (19), we find a Poisson equation for the pressure $P(t, x, y)$,

$$\nabla^2 P = -2(V_y)^2 - 2V_x U_y - NB_0^2 U_x, \tag{23}$$

with boundary conditions

$$P_y(t, x, 0) = \frac{V_{yy}(t, x, 0)}{R}, \tag{24}$$

$$P_y(t, x, 1) = \frac{V_{yy}(t, x, 1)}{R}. \tag{25}$$

The boundary conditions (24) and (25) are obtained by computing (18) at $y = 0, 1$, respectively.

2.2. Equilibrium solutions

By recalling the incompressibility condition (19) and assuming the flow fully developed along x-direction, we infer that the equilibrium profile in the y direction $V^e(y)$, which satisfies $\partial V^e/\partial y = 0$ (we use the superscript 'e' to denote the equilibrium variable). Using the boundary condition at the walls (22), we obtain that V^e must be zero. Assuming fully developed and steady state conditions, (17) reduces to

$$\frac{1}{R}\frac{\partial^2 U^e}{\partial y^2} - NB_0^2 U^e = \frac{\partial P^e}{\partial x}, \tag{26}$$

and (18) reduces to $\partial P^e/\partial y = 0$. Since the flow is assumed to be fully developed in the x direction, we conclude that $U^e = U^e(y)$, $P^e = P^e(x)$ and $\frac{\mathrm{d}P^e}{\mathrm{d}x}$ is constant. The solution of Eq. (26) is given by

$$U^e(y) = A\cosh(\sqrt{RN}B_0 y) + B\sinh(\sqrt{RN}B_0 y) - \frac{1}{NB_0^2}\frac{\mathrm{d}P^e}{\mathrm{d}x}. \tag{27}$$

Using the boundary conditions (22) at the walls we can obtain

$$A = \frac{1}{NB_0^2}\frac{\mathrm{d}P^e}{\mathrm{d}x}, \tag{28}$$

$$B = \frac{1}{NB_0^2}\frac{\mathrm{d}P^e}{\mathrm{d}x}\frac{1-\cosh(\sqrt{RN}B_0)}{\sinh(\sqrt{RN}B_0)}. \tag{29}$$

The equilibrium characterized by U^e, V^e and P^e is unstable for high Reynolds number, see [9] and references therein.

2.3. Model linearization

We define the fluctuation variables $u = U - U^e$, $v = V - V^e = V$, $p = P - P^e$, and linearize the SMHD Eqs. (17), (18) and (23) around the equilibrium profile, obtaining a new set of equations given by

$$u_t = \frac{1}{R}(u_{xx} + u_{yy}) - U^e u_x - U^e_y v - p_x - NB_0^2 u, \tag{30}$$

$$v_t = \frac{1}{R}(v_{xx} + v_{yy}) - U^e v_x - p_y, \tag{31}$$

$$p_{xx} + p_{yy} = -2U^e_y v_x - NB_0^2 u_x, \tag{32}$$

with boundary conditions

$$u(x, 0) = 0, \tag{33}$$
$$u(x, 1) = U_c(x), \tag{34}$$
$$v(x, 0) = 0, \tag{35}$$
$$v(x, 1) = V_c(x), \tag{36}$$
$$p_y(x, 0) = \frac{v_{yy}(x, 0)}{R}, \tag{37}$$
$$p_y(x, 1) = \frac{v_{yy}(x, 1) + (V_c)_{xx}(x)}{R} - (V_c)_t(x), \tag{38}$$

where $U_c(t, x, 1)$ and $V_c(t, x, 1)$ are the tangential and normal control laws implemented at the boundary $y = 1$, which are to be designed in the following section. Boundary conditions (37) and (38) are obtained by evaluating (31) at the boundaries. The continuity equation (19) is still verified

$$u_x + v_y = 0. \tag{39}$$

We use the Fourier transform on x-direction, defined as

$$f(k, y) = \int_{-\infty}^{\infty} f(x, y)\exp(-2\pi \mathrm{i}kx)\mathrm{d}x, \tag{40}$$

$$f(x, y) = \int_{-\infty}^{\infty} f(k, y)\exp(2\pi \mathrm{i}kx)\mathrm{d}k, \tag{41}$$

to transform the system equations to frequency domain. Note that we use the same symbol f for both the original $f(x, y)$ and the transformed $f(k, y)$. In the transform pair (40) and (41), k is called the wave number. The linearized model (30)–(32) written in the frequency domain is

$$u_t = \frac{1}{R}(-4k^2\pi^2 u + u_{yy}) - 2k\pi \mathrm{i}U^e u - U^e_y v - 2k\pi \mathrm{i}p - NB_0^2 u, \tag{42}$$

$$v_t = \frac{1}{R}(-4k^2\pi^2 v + v_{yy}) - 2k\pi \mathrm{i}U^e v - p_y, \tag{43}$$

$$p_{yy} = 4k^2\pi^2 p - 4k\pi \mathrm{i}U^e_y v - 2k\pi \mathrm{i}NB_0^2 u, \tag{44}$$

with boundary conditions

$$u(k, 0) = 0, \tag{45}$$
$$u(k, 1) = U_c(k), \tag{46}$$
$$v(k, 0) = 0, \tag{47}$$
$$v(k, 1) = V_c(k), \tag{48}$$
$$p_y(k, 0) = \frac{v_{yy}(k, 0)}{R}, \tag{49}$$
$$p_y(k, 1) = \frac{v_{yy}(k, 1) - 4\pi^2 k^2 (V_c)(k)}{R} - (V_c)_t(k), \tag{50}$$

where U_c, V_c are the Fourier transforms of the to-be-designed tangential and normal control laws at the boundary $y = 1$. The continuity equation (19) is transformed into the following form

$$2\pi k \mathrm{i}u(k, y) + v_y(k, y) = 0. \tag{51}$$

One of the properties of the Fourier transform, called Parseval's theorem, states that the L^2 norm in Fourier space is equal to the L^2 norm in physical space, i.e.

$$\|f\|^2_{\hat{L}^2} = \int_0^1 \int_{-\infty}^{\infty} f^2(k, y)\mathrm{d}k\mathrm{d}y = \int_0^1 \int_{-\infty}^{\infty} f^2(x, y)\mathrm{d}x\mathrm{d}y. \tag{52}$$

In Section 4, we will use this property to derive L^2 exponential stability in physical space from the same property in Fourier space. We also define the norm of $f(k, y)$ with respect to y as

$$\|f(k)\|^2_{\hat{L}^2} = \int_0^1 |f(k, y)|^2 \mathrm{d}y. \tag{53}$$

The relationship between the $\hat{L}_2$ norm and the L^2 norm is given by

$$\|f\|^2_{L^2} = \int_{-\infty}^{\infty} \|f(k)\|^2_{\hat{L}^2}\mathrm{d}k. \tag{54}$$

3. Controller design

The linearized system is spatially invariant in the x-direction and there is no coupling between different wave numbers [3]; this allows us to consider the equations for each wave number independently. It is a well-known fact [14] that there exist two wave-number bounds m and M for which the the system (42)–(51) is exponentially stable without any external control in the range $|k| \geq M$ and $|k| \leq m$. By a proper design of the control laws $U_c(k)$ and $V_c(k)$ in this section, we stabilize the system for wave numbers in the range $m < |k| < M$. The bounds m and M are estimated by the Lyapunov method in Section 4.1. We separate the controlled and uncontrolled sets mathematically using the following function

$$\chi(k) = \begin{cases} 1, & m < |k| < M \\ 0, & \text{otherwise.} \end{cases} \tag{55}$$

The transformed Poisson equation for the pressure (44) is an inhomogenous ordinary differential equation in Fourier space. Its

solution can be obtained via coefficient variation approach as follows,

$$p(k,y) = c_1\cosh(2k\pi y) + c_2\sinh(2k\pi y) + \int_0^y \left(2\mathrm{i}U^e_\xi(k,\xi)v + \mathrm{i}NB_0^2u\right)\sinh[2k\pi(\xi-y)]\mathrm{d}\xi. \quad (56)$$

Applying the boundary conditions (49) and (50) we can obtain

$$c_2 = \frac{v_{yy}(k,0)}{2k\pi R}, \quad (57)$$

$$c_1 = \frac{v_{yy}(k,1) - 4\pi^2k^2(V_c)(k)}{2k\pi R\sinh 2k\pi} - \frac{(V_c)_t(k)}{2k\pi\sinh 2k\pi} - \frac{v_{yy}(k,0)}{2k\pi R\sinh 2k\pi}\cosh 2k\pi + \int_0^1 \frac{\cosh[2k\pi(\xi-1)]}{\sinh 2k\pi}\left(2\mathrm{i}U^e_\xi(k,\xi)v + \mathrm{i}NB_0^2u\right)\mathrm{d}\xi. \quad (58)$$

Substituting $p(k,y)$ and (51) into Eq. (42) we rewrite

$$\begin{aligned} u_t = {} & \frac{1}{R}(-4k^2\pi^2u + u_{yy}) - 2k\pi\mathrm{i}U^eu - U^e_yv - NB_0^2u \\ & - 4k\pi\mathrm{i}\int_0^y U^e_\xi(k,\xi)v(k,\xi)\sinh[2k\pi(y-\xi)]\mathrm{d}\xi \\ & - 2k\pi\int_0^y NB_0^2u(k,\xi)\sinh[2k\pi(y-\xi)]\mathrm{d}\xi \\ & + \mathrm{i}\frac{\cosh[2k\pi(y-1)]}{\sinh 2k\pi}\frac{v_{yy}(k,0)}{R} \\ & + 4k\pi\frac{\cosh 2k\pi y}{\sinh 2k\pi}\int_0^1 U^e_\xi(k,\xi)v(k,\xi)\cosh[2k\pi(\xi-1)]\mathrm{d}\xi \\ & + 2k\pi\frac{\cosh 2k\pi y}{\sinh 2k\pi}\int_0^1 NB_0^2u(k,\xi)\cosh[2k\pi(\xi-1)]\mathrm{d}\xi \\ & - \mathrm{i}\frac{\cosh 2k\pi y}{\sinh 2k\pi}\left(\frac{v_{yy}(k,1) - 4k^2\pi^2V_c(k)}{R} - (V_c)_t(k)\right), \end{aligned} \quad (59)$$

with boundary conditions

$$u(k,0) = 0, \quad (60)$$

$$u(k,1) = U_c(k). \quad (61)$$

We do not need to rewrite and control the v equation (43) because using the continuity equation (51) and the fact that $v(k,0) = 0$, we can write v in terms of u

$$v(k,y) = \int_0^y v_y(k,\eta)\mathrm{d}\eta = -2k\pi\mathrm{i}\int_0^y u(k,\eta)\mathrm{d}\eta. \quad (62)$$

Thus, if u is stabilized, this dependence means that v is also stabilized. By using the continuity equation (62) and changing the order of integration, we can rewrite the second line in (59) as

$$8k^2\pi^2\mathrm{i}\int_0^y\left\{\int_\xi^y U^e_\eta(k,\eta)\sinh[2k\pi(y-\eta)]\mathrm{d}\eta\right\}u(k,\xi)\mathrm{d}\xi. \quad (63)$$

We can also change the integration order in the fifth line, and add it to the sixth line to obtain

$$\begin{aligned} & 2k\pi\frac{\cosh 2k\pi y}{\sinh 2k\pi}\int_0^1\left\{2U^e_\xi(k,\xi)\cosh[2k\pi(\xi-1)] + \mathrm{i}NB_0^2\sinh[2k\pi(1-\xi)]\right\}v(k,\xi)\mathrm{d}\xi \\ & + \mathrm{i}NB_0^2\frac{\cosh 2k\pi y}{\sinh 2k\pi}V_c(k). \end{aligned} \quad (64)$$

We now design the controllers in two steps. For the first step we define

$$\begin{aligned} (V_c)_t = {} & 2k\pi\mathrm{i}\int_0^1\left\{2U^e_\xi\cosh[2k\pi(\xi-1)] + \mathrm{i}NB_0^2\sinh[2k\pi(1-\xi)]\right\}v(k,\xi)\mathrm{d}\xi - NB_0^2V_c(k) \\ & + \frac{2k\pi\mathrm{i}\left[u_y(k,0) - u_y(k,1)\right] - 4k^2\pi^2V_c(k)}{R}, \end{aligned} \quad (65)$$

which makes (59) have a strict-feedback form [17]

$$\begin{aligned} u_t = {} & \frac{1}{R}(-4k^2\pi^2u + u_{yy}) - 2k\pi\mathrm{i}U^eu - NB_0^2u \\ & + 2k\pi\mathrm{i}U^e_y(k,y)\int_0^y u(k,\eta)\mathrm{d}\eta \\ & + 8k^2\pi^2\mathrm{i}\int_0^y\left\{\int_\xi^y U^e_\eta(k,\eta)\sinh[2k\pi(y-\eta)]\mathrm{d}\eta\right\}u(k,\xi)\mathrm{d}\xi \\ & - \int_0^y 2k\pi NB_0^2\sinh[2k\pi(y-\xi)]u(k,\xi)\mathrm{d}\xi \\ & + 2k\pi\frac{\cosh[2k\pi(y-1)] - \cosh(2k\pi y)}{\sinh 2k\pi}\frac{u_y(k,0)}{R}. \end{aligned} \quad (66)$$

For simplicity we rewrite (66) as

$$u_t = \frac{1}{R}(-4k^2\pi^2u + u_{yy}) + \lambda(k,y)u + g(k,y)u_y(k,0) + \int_0^y f(k,y,\xi)u\mathrm{d}\xi, \quad (67)$$

where

$$\lambda(k,y) = -\left(2k\pi\mathrm{i}U^e(k,y) + NB_0^2\right), \quad (68)$$

$$g(k,y) = \frac{2k\pi}{R}\frac{\cosh[2k\pi(y-1)] - \cosh(2k\pi y)}{\sinh 2k\pi}, \quad (69)$$

$$f(k,y,\xi) = 8k^2\pi^2\mathrm{i}\int_\xi^y U^e_\eta(k,\eta)\sinh[2k\pi(y-\eta)]\mathrm{d}\eta + 2k\pi\mathrm{i}U^e_y(k,y) - 2k\pi NB_0^2\sinh[2k\pi(y-\xi)]. \quad (70)$$

For the second step we note that (67) is a parabolic partial integro-differential equation and can be stabilized using the backstepping technique recently introduced in [17]. We define a backstepping tranformation,

$$\alpha = u - \int_0^y K(k,y,\eta)u(t,k,\eta)\mathrm{d}\eta, \quad (71)$$

that maps, for each wave number $k \in (m,M)$, the equation for u (66) into a heat equation

$$\alpha_t = \frac{1}{R}(\alpha_{yy} - 4k^2\pi^2\alpha), \quad (72)$$

$$\alpha(k,0) = 0, \quad (73)$$

$$\alpha(k,1) = 0, \quad (74)$$

The inverse backstepping transformation is defined as

$$u = \alpha + \int_0^y L(k,y,\eta)\alpha(t,k,\eta)\mathrm{d}\eta. \quad (75)$$

By differentiating (71) with respect to t and y (twice), and then by substituting the obtained derivatives into (72), we arrive at the following PDE for the kernel $K(y,\eta)$, in the domain $\mathcal{D} = \{(y,\eta)|0 \le \eta \le y \le 1\}$,

$$\frac{1}{R}\left[K_{yy}(y,\eta) - K_{\eta\eta}(y,\eta)\right] = \lambda(\eta)K(y,\eta) - f(y,\eta) + \int_\eta^y K(y,\xi)f(\xi,\eta)\mathrm{d}\xi, \quad (76)$$

with boundary conditions

$$K(y,y) = -\frac{R}{2}\int_0^y\lambda(\xi)\mathrm{d}\xi, \quad (77)$$

$$K(y,0) = -Rg(y) + R\int_0^y K(y,\eta)g(\eta)\mathrm{d}\eta. \quad (78)$$

We evaluate the backstepping transform (71) at the boundary $y = 1$ to obtain

$$\alpha(k,1) = u(k,1) - \int_0^1 K(k,1,\eta)u(t,k,\eta)\mathrm{d}\eta. \quad (79)$$

Then we substitute (61) and (74) into (79) to obtain the tangential control law

$$U_c = \int_0^1 K(k, 1, \eta)u(t, k, \eta)\mathrm{d}\eta. \tag{80}$$

Similarly, the equation for the inverse kernel L defined in (75) is

$$\frac{1}{R}\left[L_{yy}(y, \eta) - L_{\eta\eta}(y, \eta)\right] = -\lambda(\eta)L(y, \eta) - f(y, \eta) - \int_\eta^y L(y, \xi)f(\xi, \eta)\mathrm{d}\xi\mathrm{d}\eta \tag{81}$$

with boundary conditions

$$L(y, y) = -\frac{R}{2}\int_0^y \lambda(\xi)\mathrm{d}\xi, \tag{82}$$

$$L(y, 0) = -Rg(y). \tag{83}$$

It can be proved that both K and L equations have smooth solutions. Eqs. (76)–(78) and (81)–(83) can be solved either numerically or symbolically by using an equivalent integral equation formulation (that can be solved via a successive approximation series [17]). We now convert the control laws (65) and (80) back to the physical space via inverse Fourier transform,

$$U_c(t, x) = \int_0^1 \int_{-\infty}^{\infty} Q_u(x - \xi, \eta)u(t, \xi, \eta)\mathrm{d}\xi\mathrm{d}\eta, \tag{84}$$

$$V_c(t, x) = h(t, x), \tag{85}$$

where h verifies the parabolic equation

$$h_t = \frac{1}{R}h_{xx} - NB_0^2 h(t, x) + l(t, x), \tag{86}$$

where the function $l(t, x)$ is given by

$$l(t, x) = \int_0^1 \int_{-\infty}^{\infty} Q_v(x - \xi, \eta)v(t, \xi, \eta)\mathrm{d}\xi\mathrm{d}\eta + \int_{-\infty}^{\infty} Q_0(x - \xi)\left[u_y(t, \xi, 0) - u_y(t, \xi, 1)\right]\mathrm{d}\xi, \tag{87}$$

and the kernel Q_u, Q_v, and Q_0 are defined as,

$$Q_u(x - \xi, \eta) = \int_{-\infty}^{\infty} \chi(k)K(k, 1, \eta)\exp(2k\pi\mathrm{i}(x - \xi))\mathrm{d}k, \tag{88}$$

$$Q_v(x - \xi, \eta) = \int_{-\infty}^{\infty} \chi(k)2k\pi\mathrm{i}\{2U_\eta^e(k, \eta)\cosh[2k\pi(\eta - 1)] + \mathrm{i}NB_0^2\sinh[2k\pi(1 - \eta)]\}\exp(2k\pi\mathrm{i}(x - \xi))\mathrm{d}k, \tag{89}$$

$$Q_0(x - \xi) = \int_{-\infty}^{\infty} \chi(k)\frac{2k\pi\mathrm{i}}{R}\exp(2k\pi\mathrm{i}(x - \xi))\mathrm{d}k, \tag{90}$$

and $\chi(k)$ is defined in (55). The stable parabolic Eq. (86) determines the dynamics of the tangential controller. Due to the compatibility conditions, we let $h(0, x) = v(t, x, y)|_{t=0,y=1}$ as the initial condition. The stability results hold for $h(0, x) \neq 0$ but additional effort is required to account for the exponentially stable effect of the compensator internal dynamics.

4. Stability analysis

In Section 3, we have derived control laws for both the normal and the tangential directions at the boundary $y = 1$. In this section, we will prove the stability of the closed-loop system. Our main result is as follows at the beginning of this section. As a first step, we prove stability of the uncontrolled set of wave numbers. As a second step, we show that with the control laws in Section 3, the controlled set of wave numbers is exponentially stable. Stability in physical space follows then from stability of all wave numbers.

Theorem 1. *For the linearized system (30)–(38) with the feedback laws (84) and (85), the equilibrium profile $u(t, x, y) = v(t, x, y) = 0$ is exponentially stable in the L_2 sense:*

$$\|u(t)\|_{L^2}^2 + \|v(t)\|_{L^2}^2 \leq C_0\mathrm{e}^{\frac{-\pi^2 t}{R}}\left(\|u(0)\|_{L^2}^2 + \|v(0)\|_{L^2}^2\right), \tag{91}$$

where C_0 is defined as

$$C_0 = (1 + 4\pi^2M^2)\max_{k\in(m,M)}\{(1 + \|L\|_\infty)^2(1 + \|K\|_\infty)^2\}, \tag{92}$$

and the norm $\|\cdot\|_\infty$ is defined as $\|f\|_\infty = \max|f(y, \eta)|$.

4.1. Uncontrolled wave number analysis

For the uncontrolled system (42) and (43), we define the Lyapunov functional for each wave number k as

$$E(t) = \frac{1}{2}\int_0^1 (u\bar{u} + v\bar{v})\mathrm{d}y, \tag{93}$$

where $\bar{u}$ and $\bar{v}$ denote the complex conjugates of u and v, respectively. The time derivative of E is

$$\frac{\mathrm{d}E(t)}{\mathrm{d}t} = \int_0^1 \frac{-4k^2\pi^2}{R}(u\bar{u} + v\bar{v})\mathrm{d}y - \frac{1}{R}\int_0^1 (u_y\bar{u}_y + v_y\bar{v}_y)\mathrm{d}y - \int_0^1 NB_0^2 u\bar{u}\mathrm{d}y - \int_0^1 U_y^e\frac{u\bar{v} + \bar{u}v}{2}\mathrm{d}y. \tag{94}$$

Since N, the Stuart number, is positive, then we have

$$\frac{\mathrm{d}E(t)}{\mathrm{d}t} \leq \frac{-4k^2\pi^2}{R}\int_0^1 (u\bar{u} + v\bar{v})\mathrm{d}y - \frac{1}{R}\int_0^1 (u_y\bar{u}_y + v_y\bar{v}_y)\mathrm{d}y - \int_0^1 U_y^e\frac{u\bar{v} + \bar{u}v}{2}\mathrm{d}y. \tag{95}$$

We use Poincaré inequality [21] to find a bound for the second term in (95). Let us state the Poincaré inequality first as a lemma without proof.

Lemma 2 (*Poincaré Inequality*). *Given $f \in H$, where*

$$H = \left\{f \in C^0([0, 1])|f(0) = f(1) = 0\right\}, \tag{96}$$

with f' piecewise continuous, then

$$\|f\| \leq \frac{1}{\pi}\|f'\|, \tag{97}$$

where $\|f\|$ is given by $\|f\|^2 = \int_0^1 |f(x)|^2\mathrm{d}x$.

Lemma 2 is one of the strongest Poincaré inequality versions. Using the Poincaré inequality for the second term in (95), we obtain

$$\int_0^1 (u\bar{u} + v\bar{v})\mathrm{d}y \leq \frac{1}{\pi^2}\int_0^1 (u_y\bar{u}_y + v_y\bar{v}_y)\mathrm{d}y. \tag{98}$$

As $(u\bar{v} + \bar{u}v)$ is a real number, it satisfies $\frac{u\bar{v}+\bar{u}v}{2} = \Re(u\bar{v}) \leq |u\bar{v}| = |u||v| \leq \frac{|u|^2+|v|^2}{2}$. Therefore, taking into account (93), we can bound the time derivative of $E(t)$ in (95) as

$$\frac{\mathrm{d}E(t)}{\mathrm{d}t} \leq \left[\frac{-8k^2\pi^2}{R} - \frac{2\pi^2}{R} - \frac{\mathrm{d}U^e(1)}{\mathrm{d}y}\right]E(t). \tag{99}$$

In (99) we recalled (27) to obtain

$$U_y^e(y) = A\sqrt{RN}B_0\sinh(\sqrt{RN}B_0 y) + B\sqrt{RN}B_0\cosh(\sqrt{RN}B_0 y), \tag{100}$$

$$U_{yy}^e(y) = \frac{R}{B_0}\frac{\mathrm{d}P^e}{\mathrm{d}x}\frac{\sinh[\sqrt{RN}B_0(1 - y)] + \sinh(\sqrt{RN}B_0 y)}{\sinh(\sqrt{RN}B_0)}, \tag{101}$$

then $U_{yy}^e(y) < 0$, since $\frac{\mathrm{d}P^e}{\mathrm{d}x} < 0$ and other terms are positive for any $y \in [0, 1]$. The negativeness of the derivative $U_{yy}^e(y)$ then implies monotonicity of U_y^e on $[0, 1]$, i.e., $U_y^e(1) < U_y^e(y) < U_y^e(0)$. Therefore, we can use $U_y^e(1)$ to bound the third term in the right side of (95) and obtain (99).

Proposition 3. *For the linearized system (42)–(50), if* $m = \frac{\pi}{4R\left|\mathrm{d}U^e(1)/\mathrm{d}y\right|}$, *and* $M = \frac{1}{2\pi}\sqrt{\frac{R}{2}\left|\frac{\mathrm{d}U^e(1)}{\mathrm{d}y}\right|}$, *where* $\frac{\mathrm{d}U^e(1)}{\mathrm{d}y} = \frac{1}{B_0}\sqrt{\frac{R}{N}}\frac{\mathrm{d}P^e}{\mathrm{d}x}\frac{\cosh(\sqrt{RN}B_0)-1}{\sinh(\sqrt{RN}B_0)}$, *then for both* $|k| \le m$ *and* $|k| \ge M$, *the equilibrium* $u(t,k,y) = v(t,k,y) = 0$ *of the uncontrolled system is exponentially stable in the* L^2 *sense, i.e.*

$$\|v(t,k)\|_{\hat{L}^2}^2 + \|u(t,k)\|_{\hat{L}^2}^2 \le \mathrm{e}^{-\frac{\pi^2 t}{R}} \times \left(\|v(0,k)\|_{\hat{L}^2}^2 + \|u(0,k)\|_{\hat{L}^2}^2\right). \tag{102}$$

Proof. Taking into account that $\frac{\mathrm{d}P^e}{\mathrm{d}x} < 0$ and $\cosh(\sqrt{RN}B_0) > 1$, we can show that, for the third term in (99),

$$\frac{\mathrm{d}U^e(1)}{\mathrm{d}y} = \frac{1}{B_0}\sqrt{\frac{R}{N}}\frac{\mathrm{d}P^e}{\mathrm{d}x}\frac{\cosh(\sqrt{RN}B_0)-1}{\sinh(\sqrt{RN}B_0)} < 0. \tag{103}$$

Thus, if $|k| \ge \frac{1}{2\pi}\sqrt{\frac{R}{2}\left|\frac{\mathrm{d}U^e(1)}{\mathrm{d}y}\right|}$, then

$$\frac{\mathrm{d}E(t)}{\mathrm{d}t} \le -\frac{2\pi^2}{R}E(t). \tag{104}$$

Additionally, by using the continuity Eq. (62) we can bound (95) as

$$\frac{\mathrm{d}E(t)}{\mathrm{d}t} \le \left[\frac{-8k^2\pi^2}{R} - \frac{2\pi^2}{R} - 4|k|\pi\frac{\mathrm{d}U^e(1)}{\mathrm{d}y}\right]E(t). \tag{105}$$

Thus, if $|k| \le \frac{\pi}{4R\left|\mathrm{d}U^e(1)/\mathrm{d}y\right|}$, then

$$\frac{\mathrm{d}E(t)}{\mathrm{d}t} \le -\frac{\pi^2}{R}E(t). \tag{106}$$

Taking into account (104) and (106), and definition (93), we conclude that

$$\frac{\mathrm{d}}{\mathrm{d}t}\left(\|v(t,k)\|_{\hat{L}^2}^2 + \|u(t,k)\|_{\hat{L}^2}^2\right) \le -\frac{\pi^2}{R}\left(\|v(t,k)\|_{\hat{L}^2}^2 + \|u(t,k)\|_{\hat{L}^2}^2\right). \quad \square \tag{107}$$

In the physical space we can get similar stability property for the uncontrolled part via the Parseval's theorem:

Proposition 4. *The variables* $\epsilon_u(t,x,y)$ *and* $\epsilon_v(t,x,y)$, *defined as*

$$\epsilon_u(t,x,y) = \int_{-\infty}^{\infty}(1-\chi(k))u(t,k,y)\exp(2k\pi\mathrm{i}x)\mathrm{d}k, \tag{108}$$

$$\epsilon_v(t,x,y) = \int_{-\infty}^{\infty}(1-\chi(k))v(t,k,y)\exp(2k\pi\mathrm{i}x)\mathrm{d}k, \tag{109}$$

decay exponentially in the L^2 *sense:*

$$\|\epsilon_u(t)\|_{L^2}^2 + \|\epsilon_v(t)\|_{L^2}^2 \le \mathrm{e}^{-\frac{\pi^2 t}{R}}\left(\|\epsilon_u(0)\|_{L^2}^2 + \|\epsilon_v(0)\|_{L^2}^2\right). \tag{110}$$

Proof. Combining Proposition 3 and Parseval's theorem (52) we can prove this proposition. $\square$

4.2. Controlled wave number analysis

In this subsection, we prove the exponential stability of the linearized system with feedback control, not only in Fourier space but also in physical space, for the controlled set of wave numbers.

Proposition 5. *For any wave number* $k \in (m,M)$, *the equilibrium* $u(t,k,y) = v(t,k,y) = 0$ *of the system (42)–(50) with feedback control laws (65), (80) is exponentially stable in the* L^2 *sense, i.e.*

$$\|v(t,k)\|_{\hat{L}^2}^2 + \|u(t,k)\|_{\hat{L}^2}^2 \le C_0\mathrm{e}^{\frac{-2\pi^2 t}{R}} \times \left(\|v(0,k)\|_{\hat{L}^2}^2 + \|u(0,k)\|_{\hat{L}^2}^2\right). \tag{111}$$

Proof. For the heat equation (72), we can compute

$$\|\alpha(t,k)\|_{\hat{L}^2}^2 = \int_0^1 |\alpha(t,k,y)|^2\mathrm{d}y = \int_0^1 \alpha(t,k,y)\bar{\alpha}(t,k,y)\mathrm{d}y, \tag{112}$$

with the time derivative

$$\frac{\mathrm{d}\|\alpha(t,k)\|_{\hat{L}^2}^2}{\mathrm{d}t} = \int_0^1 \alpha_t\bar{\alpha} + \bar{\alpha}_t\alpha\mathrm{d}y \le \frac{1}{R}\int_0^1 \alpha_{yy}\bar{\alpha} + \bar{\alpha}_{yy}\alpha\mathrm{d}y = -\frac{2}{R}\int_0^1 \alpha_y\bar{\alpha}_y\mathrm{d}y \le -\frac{2\pi^2}{R}\int_0^1 \alpha\bar{\alpha}\mathrm{d}y. \tag{113}$$

Then, using Gronwall's inequality [21], we obtain $\|\alpha(t,k)\|_{\hat{L}^2}^2 \le \mathrm{e}^{\frac{-2\pi^2 t}{R}}\|\alpha(0,k)\|_{\hat{L}^2}^2$. By using (62), (71) and (75), we obtain

$$\alpha = \mathrm{i}\frac{v_y - \int_0^y K(y,\eta)v_y(t,\eta)\mathrm{d}\eta}{2k\pi}, \tag{114}$$

$$v = -2k\pi\mathrm{i}\int_0^y\left[1 + \int_\eta^y L(\eta,\xi)\mathrm{d}\xi\right]\alpha(t,\eta)\mathrm{d}\eta. \tag{115}$$

By using (75) and (115), we can obtain a bound for $\left(\|u(t,k)\|_{\hat{L}^2}^2 + \|v(t,k)\|_{\hat{L}^2}^2\right)$ in terms of $\|\alpha(0,k)\|_{\hat{L}^2}^2$, i.e.

$$\|u(t,k)\|_{\hat{L}^2}^2 + \|v(t,k)\|_{\hat{L}^2}^2 \le (1+4M^2\pi^2)(1+\|L\|_\infty)^2 \times \mathrm{e}^{-\frac{2\pi^2 t}{R}}\|\alpha(0,k)\|_{\hat{L}^2}^2. \tag{116}$$

To establish the connection between $\left(\|u(t,k)\|_{\hat{L}^2}^2 + \|v(t,k)\|_{\hat{L}^2}^2\right)$ and $\|\alpha(t,k)\|_{\hat{L}^2}$, we recall (71) as follows

$$\|\alpha(0,k)\|_{\hat{L}^2}^2 \le (1+\|K\|_\infty)^2\left(\|u(0,k)\|_{\hat{L}^2}^2 + \|v(0,k)\|_{\hat{L}^2}^2\right). \tag{117}$$

Combing (116) and (117), we finish the proof. $\square$

For the controlled part $|k| \in (m,M)$, we can obtained the following property by using Parseval's theorem:

Proposition 6. *Defining*

$$u^*(t,x,y) = \int_{-\infty}^{\infty}\chi(k)u(t,k,y)\exp(2k\pi\mathrm{i}x)\mathrm{d}k, \tag{118}$$

$$v^*(t,x,y) = \int_{-\infty}^{\infty}\chi(k)v(t,k,y)\exp(2k\pi\mathrm{i}x)\mathrm{d}k, \tag{119}$$

for the linearized system (30)–(38) with the feedback laws (84) and (85), the variables $u^*(t,x,y)$ *and* $v^*(t,x,y)$ *decay exponentially:*

$$\|u^*(t)\|_{L^2}^2 + \|v^*(t)\|_{L^2}^2 \le C_0\mathrm{e}^{-\frac{2\pi^2}{R}t} \times \left(\|u^*(0)\|_{L^2}^2 + \|v^*(0)\|_{L^2}^2\right). \tag{120}$$

Proof. Combine Proposition 5 and the Parseval's theorem (52). $\square$

By using Propositions 4 and 6 we can obtain the exponential stability of the linear system (30)–(38) over the entire wave number range, and finish the proof for Theorem 1.

4.3. Control efforts of closed-loop system

In this section, we study the control effort required to stabilize the linearized 2D MHD system. First we estimate bounds for $\|\alpha_y(t,k)\|^2_{\hat{l}^2}$ and $\|\alpha_{yy}(t,k)\|^2_{\hat{l}^2}$. We note that (72)–(74) are of heat equations and the solution $\alpha \in C^\infty([0,1]\times(0,\infty))$ if the initial value $\alpha(0,k,y) \in C([0,1])\bigcap L^\infty([0,1])$ (See Chapter 3 of [7]). Therefore, we obtain the following proposition right after the same line of (113) by using the Poincaré inequality in Lemma 2.

Proposition 7. *Defining*

$$\begin{aligned}\|\alpha_y(t,k)\|^2_{\hat{l}^2} &= \int_0^1 |\alpha_y(t,k,y)|^2\mathrm{d}y\\ &= \int_0^1 \alpha_y(t,k,y)\bar{\alpha}_y(t,k,y)\mathrm{d}y, \end{aligned} \tag{121}$$

$$\begin{aligned}\|\alpha_{yy}(t,k)\|^2_{\hat{l}^2} &= \int_0^1 |\alpha_{yy}(t,k,y)|^2\mathrm{d}y\\ &= \int_0^1 \alpha_{yy}(t,k,y)\bar{\alpha}_{yy}(t,k,y)\mathrm{d}y, \end{aligned} \tag{122}$$

then for any wave number $|k| \in (m,M)$,

$$\|\alpha_y(t,k)\|^2_{\hat{l}^2} \le \mathrm{e}^{-\frac{2\pi^2 t}{R}}\|\alpha_y(0,k)\|^2_{\hat{l}^2}, \tag{123}$$

$$\|\alpha_{yy}(t,k)\|^2_{\hat{l}^2} \le \mathrm{e}^{-\frac{2\pi^2 t}{R}}\|\alpha_{yy}(0,k)\|^2_{\hat{l}^2}, \tag{124}$$

where α solves (72)–(74).

Proof. We derive the equations of α_y and α_{yy} by taking derivatives both sides of (72)–(74). □

By using the backstepping transformations (71) and (75), we can obtain the following proposition.

Proposition 8. *For $|k| \in (m,M)$, we have the following estimates:*

$$\text{(i)}\quad \|u_y(t,k)\|^2_{\hat{l}^2} \le C_1\mathrm{e}^{-\frac{2\pi^2 t}{R}}\|u_y(0,k)\|^2_{\hat{l}^2}, \tag{125}$$

$$\text{(ii)}\quad \|u_{yy}(t,k)\|^2_{\hat{l}^2} \le C_2\mathrm{e}^{-\frac{2\pi^2 t}{R}}\|u_{yy}(0,k)\|^2_{\hat{l}^2}, \tag{126}$$

where C_1 and C_2 are positive constants.

Proof. (i) We recall the backstepping transformations (71) and (75) to compute

$$\alpha_y = u_y - K(k,y,y)u - \int_0^y K_y(k,y,\eta)u(t,k,\eta)\mathrm{d}\eta, \tag{127}$$

$$u_y = \alpha_y + L(k,y,y)\alpha + \int_0^y L_y(k,y,\eta)\alpha(t,k,\eta)\mathrm{d}\eta. \tag{128}$$

We estimate $\|\alpha_y\|_{\hat{l}^2}$ and $\|u_y\|_{\hat{l}^2}$, and then recall (123) in Proposition 7 to finish the proof.

(ii) From (71) and (75) we write the following backstepping transformations

$$\begin{aligned}\alpha_{yy} &= u_{yy} - K(k,y,y)u_y - (2K_y(k,y,y) + K_\eta(k,y,y))u\\ &\quad - \int_0^y K_{yy}(k,y,\eta)u(t,k,\eta)\mathrm{d}\eta,\\ u_{yy} &= \alpha_{yy} + L(k,y,y)\alpha_y + (2L_y(k,y,y) + L_\eta(k,y,y))\alpha\\ &\quad + \int_0^y L_{yy}(k,y,\eta)\alpha(t,k,\eta)\mathrm{d}\eta,\end{aligned}$$

and use similar arguments to those used in the proof of i) to complete the proof. □

Theorem 9. *The feedback controls U_c, V_c are L^2 functions of x.*

Proof. We first consider the expression of the tangential control which is defined by $U_c = \int_0^1 K(k,1,\eta)u(t,k,\eta)\mathrm{d}\eta$, then

$$\begin{aligned}\|U_c\|^2_{L^2} &= \int_{-\infty}^{\infty} U_c(t,x)^2\mathrm{d}x = \int_{-\infty}^{\infty}|U_c|(t,k)^2\mathrm{d}k\\ &= \int_{-\infty}^{\infty}\chi(k)\left|\int_0^1 K(k,1,\eta)u(t,y,k)\mathrm{d}\eta\right|^2\mathrm{d}k\\ &\le 2(M-m)\max_{m\le|k|\le M}\{\|K\|_\infty\}\|u\|^2_{L^2}.\end{aligned} \tag{129}$$

For the tangential control V_c, we take into account the controller dynamics determined by (85)–(87). We consider the parabolic system (86)–(87) with the initial value $h(0,x) = h_0(x)$, where $l(t,x)$ is already indicated by the Eq. (87). Then we compute the Fourier transform of $l(t,x)$ with respect to x, $l(t,k) = \tilde{A}(t,k) + \tilde{B}(t,k) + \tilde{C}(t,k)$, where

$$\tilde{A}(t,k) = 4k\pi\mathrm{i}\int_0^1 U^e_\xi\cosh[2k\pi(\xi-1)]v(t,k,\xi)\mathrm{d}\xi, \tag{130}$$

$$\tilde{B}(t,k) = -2k\pi NB_0^2\int_0^1\sinh[2k\pi(1-\xi)]v(t,k,\xi)\mathrm{d}\xi, \tag{131}$$

$$\tilde{C}(t,k) = \frac{2k\pi\mathrm{i}[u_y(t,k,0) - u_y(t,k,1)]}{R}. \tag{132}$$

Finally, we obtain the following estimates:

$$|l(t,k)|^2 \le 3(|\tilde{A}|^2 + |\tilde{B}|^2 + |\tilde{C}|^2).$$

Using Cauchy–Schwarz inequality, we can obtain

$$|l(t,k)|^2 \le C_3\|v(t,k,\cdot)\|^2_{\hat{l}^2} + C_4\|u_{yy}(t,k,\cdot)\|^2_{\hat{l}^2}, \tag{133}$$

where C_3, C_4 are positive constants. We use Propositions 5 and 8 to bound the right hand terms in (133) and to obtain

$$|l(t,k)|^2 \le \left(C_5\|v(0,k,\cdot)\|^2_{\hat{l}^2} + C_6\|u_{yy}(0,k,\cdot)\|^2_{\hat{l}^2}\right)\mathrm{e}^{-\frac{2\pi^2 t}{R}}, \tag{134}$$

where C_5, C_6 are positive constants. Integrating (134) in k over $(|k| \in [m,M])$ we obtain

$$\|l(t)\|^2_{L^2} \le \left(C_5\|v(0)\|^2_{L^2} + C_6\|u_{yy}(0)\|^2_{L^2}\right)\mathrm{e}^{-\frac{2\pi^2 t}{R}}. \tag{135}$$

We now define $\mathcal{A}$ as $\mathcal{A}\xi = \frac{\xi_{xx}}{R} - NB_0^2\xi$ on $\mathcal{D}(\mathcal{A}) = \{\xi \in H^1(\mathbb{R})|\xi(t,\pm\infty) = 0\}$. Thus, $\mathcal{A}$ is a generator of a strongly continuous semigroup (C_0-semigroup) $\{S(t)\}$, and $\|S(t)\| \le C\mathrm{e}^{-\frac{\omega}{2}t}$, $t \ge 0$ for some C, $\omega > 0$ [12]. We can set $\omega = 2\left(\frac{\pi^2}{R} + NB_0^2\right)$ due to the following estimate

$$\begin{aligned}\frac{1}{2}\frac{\mathrm{d}}{\mathrm{d}t}\int_{\mathbb{R}}|\xi|^2\mathrm{d}x &= \int_{\mathbb{R}}\xi\left(\frac{1}{R}\xi_{xx} - NB_0^2\xi\right)\mathrm{d}x\\ &= \frac{1}{R}\xi\xi_x\Big|_{-\infty}^{\infty} - \frac{1}{R}\int_{\mathbb{R}}\xi_x^2\mathrm{d}x - NB_0^2\int_{\mathbb{R}}\xi^2\mathrm{d}x\\ &\le -\left(\frac{\pi^2}{R} + NB_0^2\right)\int_{\mathbb{R}}\xi^2\mathrm{d}x.\end{aligned} \tag{136}$$

By using Gronwall's inequality we can obtain

$$\|\xi(t,\cdot)\|^2_{L^2} \le \mathrm{e}^{-2\left(\frac{\pi^2}{R}+NB_0^2\right)t}\|\xi(0,\cdot)\|^2_{L^2}.$$

We let $h(t,x) = h_0(x)$, then we have

$$\begin{aligned}\|h(t,\cdot)\|^2_{L^2} &= \left\|S(t)h_0(x) + \int_0^t S(t-\tau)l(\tau,\cdot)\mathrm{d}\tau\right\|^2_{L^2}\\ &\le \|S(t)h_0(x)\|_{L^2} + \int_0^t\|S(t-\tau)l(\tau,\cdot)\|^2_{\hat{l}^2}\,\mathrm{d}\tau\\ &\le C^2\mathrm{e}^{-\omega t}\|h_0\|^2_{\hat{l}^2} + \int_0^t C^2\mathrm{e}^{-\omega(t-\tau)}\mathrm{e}^{-\frac{2\pi^2}{R}\tau}\end{aligned}$$

$$\times \left(C_5\|v(0)\|_{L^2}^2 + C_6\|u_{yy}(0)\|_{L^2}^2\right) \mathrm{d}\tau$$
$$= C^2\|h_0\|_{L^2}^2 \mathrm{e}^{-\omega t} + \frac{C^2C_5\|v(0)\|_{L^2}^2 + C^2C_6\|u_{yy}(0)\|_{L^2}^2}{2NB_0^2}$$
$$\times \mathrm{e}^{-\frac{2\pi^2}{R}} \left(1 - \mathrm{e}^{-2NB_0^2 t}\right). \quad (137)$$

Then we conclude that $V_c(t, x) = h(t, x)$ is a L^2 function of x and

$$\lim_{t\to\infty} \|h(t)\|_{L^2}^2 = 0. \quad \square \quad (138)$$

5. Conclusions and future work

We have designed backstepping-based boundary feedback controllers which exponentially stabilize the 2D magnetohydrodynamic equations linearized around a Hartmann equilibrium profile in the L^2 sense. The results have been presented in 2D for ease of notation. Since 3D channels are spatially invariant in both streamwise and spanwise direction, the design can be extended to 3D by applying the Fourier transform in both invariant directions and following similar steps. It is also worth mentioning that the design can be extended to periodic channel flow, both in 2D and 3D, by substituting the Fourier transform by a Fourier series.

The controllers derived in this work are written as state feedback. An observer has been developed based on [18], and is presented in [23]. DNS simulations will be carried out to show the performance of this feedback controller in 3D.

Acknowledgement

We thank Jennie Cochran for helpful discussions and for reviewing the paper.

References

[1] C. Airau, M. Castets, On the amplification of small disturbances in a channel flow with a normal magnetic field, Physics of Fluids 16 (2004) 2991–3005.
[2] J. Baker, A. Armaou, P. Christofides, Drag reduction in transitional linearized channel flow using distributed control, International Journal of Control 75 (15) (2002) 1213–1218.
[3] B. Bamieh, F. Paganini, M.A. Dahleh, Distributed control of spatially-invariant systems, IEEE Transactions on Automatic Control 45 (2000) 1091–1107.
[4] T.W. Berger, J. Kim, C. Lee, J. Lim, Turbulent boundary layer control utilizing the Lorentz force, Physics of Fluids 12 (2000) 631.
[5] H. Choi, P. Moin, J. Kim, Active turbulence control for drag reduction in wall-bounded flows, Journal of Fluid Mechanics 262 (1994) 75.
[6] J. Cochran, R. Vazquez, M. Krstic, Backstepping boundary control of Navier–Stokes channel flow: A 3D extension, in: 2006 American Control Conference, Minneapolis, Minnesota, 2006.
[7] L.C. Evans, Partial Differential Equations, in: Graduate Studies in Mathematics, vol. 19, American Mathematical Society Providence, RI, 2002.
[8] J. Hartmann, Theory of the laminar flow of an electrically conductive liquid in a homogeneous magnetic field, Det Kgl. Danske Vidensk-abernes Selskab Mathematisk-fysiske Meddelelser XV (6) (1937) 1–27.
[9] D.S. Krasnov, E. Zienicke, O. Zikanov, T. Boeck, A. Thess, Numerical study of the instability of the Hartmann layer, Journal of Fluid Mechanics 504 (2004) 183–211.
[10] D. Lee, H. Choi, Magnetohydrodynamic turbulent flow in a channel at low magnetic reynolds number, Journal of Fluid Mechanics 439 (2001) 367–397.
[11] R.C. Lock, The stability of the flow of an electrically conducting fluid between parallel planes under a transverse magnetic field, Proceedings of Royal Society of London A 233 (1955) 105.
[12] A. Pazy, Semigroups of Linear Operators and Applications to Partial Differential Equations, Springer, New York, 1983.
[13] M.C. Potter, J.A. Kutchey, Stability of plane Hartmann flow subject to a transverse magnetic field, Physics of Fluids 16 (11) (1848).
[14] P.J. Schmid, D.S. Henningson, Stability and Transition in Shear Flows, Springer, New York, 2001.
[15] E. Schuster, M. Krstic, Inverse optimal boundary control for mixing in magnetohydrodynamic channel flows, in: 42th IEEE Conference on Decision and Control, 2003.
[16] S.N. Singh, P.R. Bandyopadhyay, Linear feedback control of boundary layer using electromagnetic microtiles, Transactions of ASME 119 (1997) 852–858.
[17] A. Smyshlyaev, M. Krstic, Closed form boundary state feedbacks for a class of partial integro-differential equations, IEEE Transactions on Automatic Control 49 (2004) 2185–2202.
[18] A. Smyshlyaev, M. Krstic, Backstepping observers for parabolic PDEs, Systems and Control Letters 54 (2005) 1953–1971.
[19] E. Spong, J.A. Reizes, E. Leonardi, Efficiency improvements of electromagnetic flow control, Heat and Fluid Flow 26 (2005) 635–655.
[20] M. Takashima, The stability of the modified plane Poisseuille flow in the presence of a transverse magnetic field, Fluid Dynamics Research 17 (1996) 293–310.
[21] A. Tveito, R. Winther, Introduction to Partial Differential Equations: A Computational Approach, in: Texts in Applied Mathematics, vol. 29, Springer-Verlag, New York, 1998.
[22] R. Vazquez, M. Krstic, A closed-form feedback controller for stabilization of linearized Navier–Stokes equations: The 2D Poisseuille flow, in: 45th IEEE Conference on Decision and Control, Seville, Spain, 2005.
[23] R. Vazquez, E. Schuster, M. Krstic, A closed-form observer for the 3D inductionless MHD and Navier–Stokes channel flow, in: 46th IEEE Conference on Decision and Control, San Diego, CA, 2006.
[24] V. Vladimirov, K. Ilin, The three-dimensional stability of steady MHD flows of an ideal fluid, Physics of Plasmas 5 (12) (1998) 4199–4204.